Theoretical simulation of temperature distribution in the brain during mild hypothermia treatment for brain injury

L. Zhu C. Diao

Department of Mechanical Engineering, University of Maryland Baltimore County, Baltimore, USA

Abstract—*Mild or moderate hypothermia (>30 °C) has been proposed for clinical use as a therapeutic option for achieving protection from cerebral ischaemia in brain injury patients. In this research, a theoretical model was developed to examine the brain temperature gradients during selective cooling of the brain surface after head injury. The head was modelled as a hemisphere consisting of several layers, representing the scalp, skull and brain tissue, respectively. The dimensions, physical properties and physiological characteristics for each layer, as well as the arterial blood temperature, were used as the input to the Pennes bioheat transfer equation to simulate the steady-state temperature distribution within the brain. Depending on the head surface temperature, a temperature gradient of up to 13 °C exists in the brain tissue. The results have shown that the volumetric-averaged brain tissue temperature $T_{bt,avg}$ for adults and infants can be 1.7 and 4.3 °C, respectively, lower than the temperature of the arterial blood supplied to the brain tissue. The location where the probe should be placed to measure $T_{bt,avg}$ was also determined by the simulation. The calculation suggests that the temperature sensor should be placed 7.5 mm and 5.9 mm beneath the brain tissue surface for adults and infants, respectively, to monitor $T_{bt,avg}$ continuously.*

Keywords—*Bioheat transfer, Mild hypothermia, Temperature, Brain, Simulation, Brain injury*

Med. Biol. Eng. Comput., 2001, **39**, 681–687

1 Introduction

IN RECENT years, mild or moderate hypothermia (>30 °C) has been proposed for clinical use as an adjunct for achieving protection from cerebral ischaemia (BARONE *et al.*, 1997; MARION *et al.*, 1996; SIRIMANNE *et al.*, 1996) and traumatic brain injury (MARION, 1997). In contrast to systemic cooling, which can produce deleterious systemic effects, selectively cooling the brain surface alone has attracted considerable attention. Experimental studies have demonstrated that mild or moderate hypothermia reduces mortality compared with normothermia or hyperthermia in rats after fluid-percussion injury (CLIFTON *et al.*, 1991) and severe controlled cortical impact (CLARK *et al.*, 1996). It has been shown that a reduction in brain temperature as small as 2 °C reduced ischaemic cell damage (CLARK *et al.*, 1996) or significantly improved post-ischaemic regional histopathology (WASS *et al.*, 1995).

Most experimental studies suggest that, during mild to moderate hypothermia, it is important to monitor closely both the brain and body core temperature (WASS *et al.*, 1995). For clinical purposes, brain temperature in patients at risk of ischaemic brain injury is not usually monitored directly because of concern about inducing additional tissue damage by the introduction of temperature probes. Current non-invasive temperature measurements, such as MRI, lack the resolution to monitor the small (±2 °C) temperature variations of interest. It is usually assumed clinically that brain temperature is equal to body core temperature.

Measurements have demonstrated that the body temperature of rats does not always reflect brain temperature (JIANG *et al.*, 1991), and a significant disparity of up to 5 °C has been reported (BARONE *et al.*, 1997; MELLERGARD *et al.*, 1990; SCHWAB *et al.*, 1997; VERLOOY *et al.*, 1995). Knowing the temperature difference between brain and core temperatures is clinically valuable.

Even though human brain temperature has been directly monitored in several clinical studies (RUMANA *et al.*, 1998; STONE *et al.*, 1997), the placement of the temperature probes was still a methodological problem, because there could be significant temperature variations within the regions of the brain (GINSBERG and BUSTO, 1998; STONE *et al.*, 1995; WASS *et al.*, 1998). During surface cooling, ambient or brain surface temperature will produce an artifact in the brain temperature measurement if the probe is placed in the superficial region. Furthermore, it has been shown that the temporal muscle temperature underestimated brain temperature by as much as 4 °C during global forebrain ischaemia of rats (KULUZ *et al.*, 1992; MIYAZAWA and HOSSMANN, 1992).

Temporal and spatial temperature gradients in the brain during hypothermia depend on heat convection due to blood flow, heat conduction through the tissue and metabolic heat generation in the heat balance. The size of the brain can play a significant role in the temperature gradient by affecting heat conduction. For

Correspondence should be addressed to Dr L. Zhu; email: zliang@umbc.edu

Paper received 2 October 2000 and in final form 30 August 2001

MBEC online number: 20013618

example, the brains of infants are considerably smaller than those of adults. DEXTER and HINDERMAN (1994) showed that conduction has a moderate effect on the brain temperature of infants, compared with little effect on that of adults. The animal models currently used in clinical studies also have smaller brains than those of typical adults. Thus temperature distributions measured in animal models may not apply directly to human brains. Consequently, it is not clear whether the protection effects achieved in animal models are applicable to humans.

In contrast to numerous clinical and experimental studies on hypothermia of the brain, there are only a few theoretical studies that have examined the temporal and spatial temperature gradient in the human brain. NELSON and NUNNELEY (1998) calculated the steady-state temperature distribution during normal and hyperthermic conditions and found that the temperature within the brain is uniform, except for the region close to the brain surface.

DEXTER and HINDERMAN (1994) developed a one-dimensional model for brain cooling during cardiopulmonary bypass (CPB). It examined the effects of different mechanisms (conduction, convection and metabolism) on the cooling rate of the brain and showed that, under the circumstances of CPB, the convective effect due to blood flow is the dominant mode of cerebral cooling in both adults and infants. The temperature distribution was assumed uniform in the brain. Thus this model cannot predict regional brain temperature variation.

An earlier model by OLSEN *et al.* (1985) simulated the temperature distribution in a monkey head during CPB. They focused on temperature distribution in the head during and before CPB. Another mathematical model for the human brain was developed by XU *et al.* (1999) to simulate the brain temperature distribution during cold-water submersion, in which the boundary condition is different from surface cooling. These theoretical models either are too simple to model the regional temperature distribution or do not consider the temperature-dependent properties. In addition, the appropriate position of an intracerebral thermal sensor has never been addressed in these studies. A comprehensive theoretical model considering the temperature-dependent properties and blood flow is still needed to examine the temperature gradients in the human brain during surface cooling.

In this study, we developed a theoretical model to examine steady-state brain temperature gradients during selective cooling of the brain. The Pennes bioheat equation was used to model the steady-state heat transfer inside the brain during surface cooling. Local temperature-dependent cerebral blood flow, metabolic heat generation and arterial blood temperature were then incorporated into the theoretical model so that the temperature field could be examined. Parametric studies were conducted to show the thermal effects of CBF, surface temperature and brain size on the temperature gradient. Since the volumetric-averaged brain tissue temperature $T_{bt,avg}$ may be associated with patients' outcomes, the location where the probe should be placed to measure $T_{bt,avg}$ was determined by the simulation. Furthermore, the factors that could be related to the average brain temperature and body core temperature were evaluated.

2 Mathematic formulation

Unlike a purely conductive medium, heat transport in perfused tissue is difficult to model, because the convective effects of the blood flow are not readily assessed. Blood vessels are present in such large numbers and have such a complicated geometry that it is not practical to develop a comprehensive model that includes the effects of all thermally significant vessels in a tissue. Existing models of heat transport in tissue include continuum models, in which the heat and mass transport effects are averaged over a representative control volume.

One of the widely used continuum models was proposed by PENNES (1948) and is given by

$$\rho c \frac{\partial T_t}{\partial t} = \Delta k_t \cdot \Delta T_t + \rho c \omega (T_a - T_t) + q_m \tag{1}$$

where k_t is the thermal conductivity of tissue, ρ is the blood density, c is the specific heat of blood, ω is the local blood perfusion rate, and q_m is the local metabolic heat generation rate. T_t is tissue temperature, and T_a is arterial blood temperature. Originally applied to predict temperature fields in the human forearm, this equation is a relatively simple modification of the ordinary heat conduction equation, obtained by adding the last two terms on the right-hand side. In the first, the moving blood contribution is treated as an isotropic heat source/sink, and the second accounts for metabolic heat production. The isotropic heat source/sink term is assumed to be proportional to the local blood perfusion rate and the difference between the arterial blood and local tissue temperature.

Many researchers have questioned the validity of the Pennes equation since 1980. Nevertheless, it has been successfully applied as an analytical tool for bioheat transfer analyses. Successes include its implementation in mathematical simulations of procedures such as therapeutic hyperthermia for the treatment of cancer and estimation of a blood perfusion rate from experimentally measured local temperature gradients and heat flows. With an adjustable blood perfusion rate, the Pennes equation has been used to predict the temperature distribution in kidney cortexes (KOLIOS *et al.*, 1998), in canine prostates (ZHU and XU, 1999) and in the brain (LYONS *et al.*, 1989; SAMULSKI *et al.*, 1989), and good agreements with experimental results have been obtained for these tissues.

In this analysis, the brain is modelled as a hemisphere of cerebral tissue with uniformly thick layers of skull and scalp. Each component is assigned appropriate dimensions, as listed is Table 1. It has been shown by previous measurements that the male brain has an average volume of 1200 ml, a length of 165 mm and a width of 140 mm (BLINKOV and GLEZER, 1968). The dimensions of the hemisphere in our model were selected to match the realistic values.

As thermal conductivity and diffusivity can be quite different for skin, muscle, bone and brain tissue, the brain is assumed to consist of three distinct layers, as shown in Fig. 1. The first layer represents the scalp. The second layer represents the skull. The brain tissue, consisting of both grey and white matter, is represented by the inside hemisphere. Brain grey matter and white matter have similar thermal properties, and therefore the brain tissue is assumed to have homogeneous thermal properties. Assuming homogeneous thermal properties within each layer, the Pennes bioheat transfer equation in spherical co-ordinates can be written as

$$\begin{aligned} k_{st,bone,bt} \frac{1}{r^2} \left[\frac{\partial}{\partial r} \left(r^2 \frac{\partial T_{sc,bone,bt}}{\partial r} \right) \right. \\ \left. + \frac{1}{\sin\theta} \frac{\partial}{\partial \theta} \left(\sin\theta \frac{\partial T_{sc,bone,bt}}{\partial \theta} \right) \right] \\ + (\rho c)_{blood} \omega (T_a - T_{sc,bone,bt}) + q_m = 0 \end{aligned} \tag{2}$$

where subscripts *sc*, *bone* and *bt* represent scalp, bone and brain tissue layers, respectively. T_a is the temperature of the arterial blood supplied to the brain.

At the interfaces between the scalp and bone, and between the bone and brain tissue, temperature and heat flux continuities are required. At the bottom of the hemisphere, an adiabatic condition is prescribed. This adiabatic condition is reasonable, as most of the heat transfer occurs in the radial direction from the inside

Table 1 Physical and physiological properties in the model

Parameter		Symbol	Value	References
Specific heat, $W\,kg^{-1}\,K^{-1}$	blood	c_{blood}	3800	DEXTER and HINDERMAN, 1994
	scalp	c_{sc}	4000	XU *et al.*, 1999
	bone	c_{bone}	2300	
	brain tissue	c_{bt}	3700	
Mass density, $kg\,m^{-3}$	blood	ρ_{blood}	1050	OLSEN *et al.*, 1985
	scalp	ρ_{sc}	1000	
	bone	ρ_{bone}	1500	
	brain tissue	ρ_{bt}	1050	
Thermal conductivity, $W\,mK^{-1}$	scalp	k_{sc}	0.34	OLSEN *et al.*, 1985
	bone	k_{bone}	1.16	
	brain tissue	k_{bt}	0.50	
Perfusion rate (normal), $ml\,100\,g^{-1}\,min^{-1}$	scalp	ω_{sc}	2.0	NELSON and NUNNELEY, 1998
	bone	ω_{bone}	1.8	XU *et al.*, 1999
	brain tissue	ω_{bt}	50	
Metabolic heat generation rate (normal), $W\,m^{-3}$	scalp	$q_{m,sc}$	363.4	XU *et al.*, 1999
	bone	$q_{m,bone}$	368.3	
	brain tissue	$q_{m,bt}$	10437	
Thickness (adult), mm	scalp	r_3–r_2	4	DEXTER and HINDERMAN, 1994
	bone	r_2–r_1	4	NELSON and NUNNELEY, 1998
	brain tissue	r_1	85	
Thickness (infant), mm	scalp	r_3–r_2	2	DEXTER and HINDERMAN, 1994
	bone	r_2–r_1	2	
	brain tissue	r_1	53	

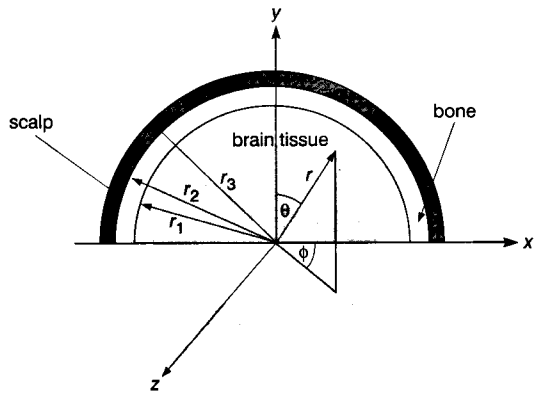

Fig. 1 *Schematic diagram of the brain cooling model and co-ordinate system*

of the brain to the surface during brain surface cooling, although this boundary condition is not strictly satisfied. Cooling of the brain can be induced by either cold fluid flowing around the brain surface or ice packed outside the brain. Considering the geometric symmetry of the model, we can assume a uniform temperature at the brain surface. Therefore the boundary condition at the brain surface is a prescribed temperature. The boundary conditions are given by

$$
\begin{aligned}
&r = 0, && \frac{\partial T_{bt}}{\partial r} = 0 \\
&r = r_3, && T_{sc} = T_{skin} \\
&r = r_2, && T_{sc} = T_{bone}, \quad k_{sc}\frac{\partial T_{sc}}{\partial r} = k_{bone}\frac{\partial T_{bone}}{\partial r} \\
&r = r_1, && T_{bone} = T_{bt}, \quad k_{bone}\frac{\partial T_{bone}}{\partial r} = k_{bt}\frac{\partial T_{bt}}{\partial r} \\
&\theta = \frac{\pi}{2}, && \frac{\partial T_{sc,bone,bt}}{\partial \theta} = 0
\end{aligned}
\qquad (3)
$$

Using the governing equation and boundary conditions given above, a computational algorithm has been developed using the finite difference method and Gauss–Siedel iteration. A uniform grid size of 0.1 mm was used in the radial direction. Based on the algorithm, a FORTRAN code was written and run on a multiprocessor computer system. The program was tested to ensure that variations in the grid size or the number of iterations would yield less than 1% change in the final results.

3 Results

Table 1 lists the geometric parameters depicting the anatomical details of the modelled brain and the physical thermal properties of the tissue. The physiological parameters, such as blood perfusion rate and metabolic heat generation under normal conditions, are also given in this Table. In this study, temperature distribution within the brain was simulated for both the adult brain and infant brain, based on the parameters given in Table 1. The influence of the head surface temperature T_{skin}, the temperature of the arterial blood supplied to the brain T_a and the local blood perfusion rate in the brain tissue ω_{bt} on the temperature field was evaluated, respectively. In each simulation, only one of the three parameters (T_{skin}, T_a and ω_{bt}) varied, and all the other parameters provided by Table 1 were fixed.

Fig. 2 gives the temperature distributions in an adult brain under different head surface cooling temperatures ($T_{skin} = 0\,°C$, $10\,°C$, $20\,°C$ and $30\,°C$) when T_a is $37\,°C$. Note that all the geometric and thermal physical properties used in the simulation are given in Table 1. The simulation predicts that the brain temperature decays in the radial direction from a temperature slightly higher ($0.3\,°C$) than T_a to the surface cooling temperature. Most of the temperature decay occurs in the bone and scalp layers. Temperature variation in the brain tissue layer is limited to the superficial area of the brain tissue surface where $T_b - T_{bt} > 0.2\,°C$ ($\Delta r = 17$ mm against $r_1 = 85$ mm). Depending on the head surface temperature, a temperature gradient of up to $13\,°C$ exists in the brain tissue.

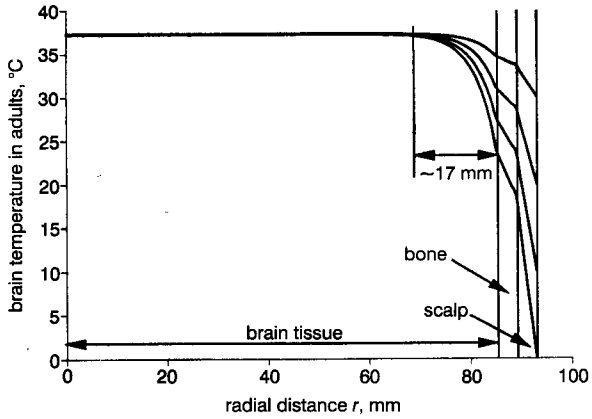

Fig. 2 *Radial temperature distribution in adult brain for different surface cooling temperatures. Uniform blood perfusion in each layer; $T_a = 37\,°C$*

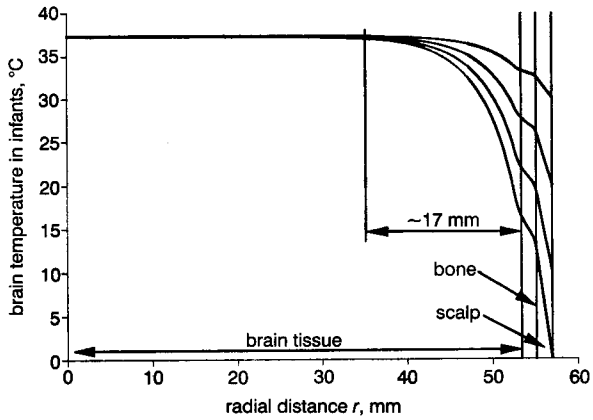

Fig. 3 *Radial temperature distribution in infant brain for different surface cooling temperatures. Uniform blood perfusion in each layer; $T_a = 37\,°C$*

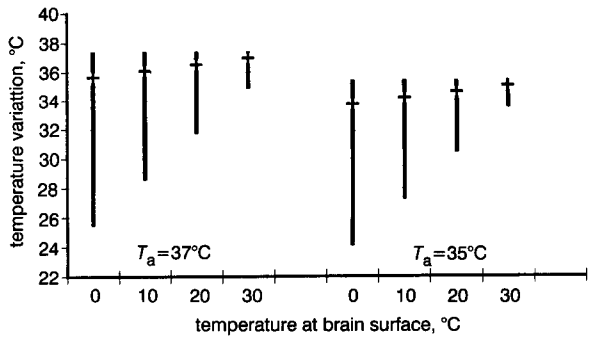

Fig. 4 *Effects of head surface temperature and arterial blood temperature on maximum, minimum and average brain tissue temperature in adults. (+) Average temperature*

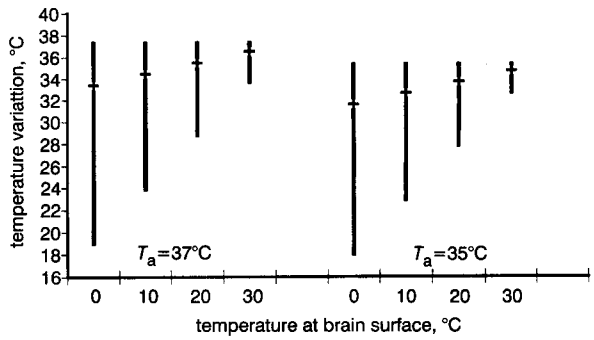

Fig. 5 *Effects of head surface temperature and arterial blood temperature on maximum, minimum and average brain tissue temperature in infants. (+) Average temperature*

Temperature distribution in an infant brain is similar to that in an adult brain, except that a larger temperature gradient (up to 20 °C) exists in the brain tissue area, as shown in Fig. 3. This is reasonable, as the infant has a smaller brain size and smaller conductive heat resistance. Even if the temperature variation occurs in the area close to the brain tissue surface, the percentages of brain tissue volumes with temperature variation for adults and infants are more than 49% and 63%, respectively.

The maximum, minimum and average temperatures of the brain tissue for different head surface temperatures and arterial blood temperatures are shown in Figs 4 and 5. The volumetric-averaged brain tissue temperature $T_{bt,avg}$ was calculated from the radial temperature distribution. The resulting deviations between $T_{bt,avg}$ and T_a for adults and infants are found to be 1.7 °C and 4.3 °C, respectively, when the head surface is 0 °C (Table 2). On the other hand, under normal conditions when the head surface is around 30 °C, the average brain tissue temperatures are only 0.4 °C and 0.9 °C lower than the deep brain temperature.

Figs 4 and 5 also examine the effect of arterial blood temperature. As shown in ZHU (2000), the temperature difference between the body core and arterial blood supplied to the brain could be as much as 2 °C if the neck surface is packed with ice. Thus, 35 °C is the possible lower limit of the arterial blood temperature used in the simulation. We have found that arterial blood temperature has a minor effect on the shape of the radial temperature distribution. However, a lower T_a of 35 °C leads to an almost uniform temperature decrease of 2 °C in the entire brain tissue layer, in comparison with the situation when T_a is 37 °C.

Table 2 Average brain tissue temperature for different ω, T_a, T_{skin}, and brain sizes

	ω_{bt} ml min^{-1} 100 g^{-1}		25	50	100	50 $3^{(T-T_a)/10}$
$T_{bt,avg}$	adult	$T_{skin} = 30\,°C$	36.9 °C	36.9 °C	36.9 °C	36.9 °C
	$T_a = 37\,°C$	$T_{skin} = 20\,°C$	36.1 °C	36.4 °C	36.6 °C	36.3 °C
		$T_{skin} = 10\,°C$	35.2 °C	35.9 °C	36.3 °C	35.6 °C
		$T_{skin} = 0\,°C$	34.4 °C	35.3 °C	36.0 °C	34.8 °C
	infant	$T_{skin} = 30\,°C$	36.2 °C	36.4 °C	36.6 °C	36.4 °C
	$T_a = 37\,°C$	$T_{skin} = 20\,°C$	34.3 °C	35.2 °C	35.8 °C	35.0 °C
		$T_{skin} = 10\,°C$	32.4 °C	34.0 °C	35.0 °C	32.9 °C
		$T_{skin} = 0\,°C$	30.5 °C	32.7 °C	34.3 °C	30.4 °C

In Table 1, $\omega_{bt} = 50\,\text{ml}\,\text{min}^{-1}\,100\,\text{g}^{-1}$ is considered as the blood perfusion rate in brain tissue during normal conditions. In this study, simulations were performed when the value of ω_{bt} was decreased or increased by 50% of its normal value. In addition, another simulation was conducted when ω_{bt} was considered as temperature-dependent. If we assume that the local blood perfusion rate is coupled with the local metabolic heat generation, the temperature-dependent ω_{bt} could be proposed as

$$\omega_{bt} = \omega_{bt,0} 3^{(T_{br}-T_a)/10} \tag{4}$$

where $\omega_{bt,0}$ is the blood perfusion rate under normal conditions ($50\,\text{ml}\,\text{min}^{-1}\,100\,\text{g}^{-1}$). The influence of blood perfusion rate of the brain tissue on the radial temperature distribution is illustrated in Figs 6 and 7. It is noted that the small blood perfusion rate in the brain tissue shifts the cool region toward the brain centre. The heavy solid line in Figs 6 and 7 represents the temperature distribution when the blood perfusion rate is temperature-dependent and this dependence is given by eqn 4.

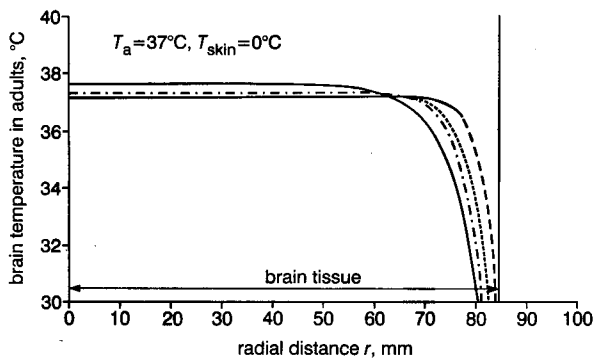

Fig. 6 *Radial temperature distributions in adult brain for different blood perfusion rates. (——) $\omega_{bt} = 25\,\text{ml}\,\text{min}^{-1}\,100\,\text{g}^{-1}$; (· · ·) $\omega_{bt} = 50\,\text{ml}\,\text{min}^{-1}\,100\,\text{g}^{-1}$; (– – –) $\omega_{bt} = 100\,\text{ml}\,\text{min}^{-1}\,100\,\text{g}^{-1}$; (– · – ·) temperature-dependent ω_{bt}*

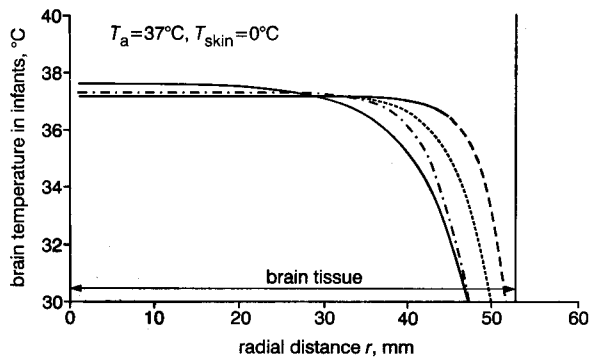

Fig. 7 *Radial temperature distributions in an infant brain for different blood perfusion rates. (——) $\omega_{bt} = 25\,\text{ml}\,\text{min}^{-1}\,100\,\text{g}^{-1}$; (· · ·) $\omega_{bt} = 50\,\text{ml}\,\text{min}^{-1}\,100\,\text{g}^{-1}$; (– – –) $\omega_{bt} = 100\,\text{ml}\,\text{min}^{-1}\,100\,\text{g}^{-1}$; (– · – ·) temperature-dependent ω_{bt}*

It is observed that the temperature curve approaches the $50\,\text{ml}\,\text{min}^{-1}\,100\,\text{g}^{-1}$ curve in the central region where the temperature is close to 37 °C, while it approaches the $25\,\text{ml}\,\text{min}^{-1}\,100\,\text{g}^{-1}$ curve in the superficial region where the local temperature is significantly lower than 37 °C. The average brain tissue temperature in adults and infants can be 2.2 °C and 6.5 °C, respectively, lower than T_a if the blood perfusion rate is allowed to decrease with the local tissue temperature.

During hypothermia treatment, it is important to continuously monitor the intracerebral temperature. If the average brain tissue temperature is associated with the patient outcome after hypothermia therapy, it is valuable to identify the locations reflecting $T_{bt,avg}$. Tables 3 and 4 give the location of the average brain tissue temperature under different conditions. This location is a function of the local blood perfusion rate and the head size. It is independent of T_a and T_{skin}. It shows that under the simulated conditions using the parameters listed in Table 1, the temperature sensor monitoring the average brain tissue temperature should be placed 7.5 mm and 5.9 mm beneath the brain tissue surface (or 15.5 mm and 9.9 mm beneath the head skin) for adults and infants, respectively.

4 Discussion

During hypothermia treatment of brain injury, it would be useful to know whether adequate cerebral hypothermia has been achieved. Mild hypothermia for brain injury is usually defined as a brain temperature ranging from 32 to 36 °C. It has been known to be protective in terms of performance, neurological function, and brain morphology. Experimental studies on rats have shown that the threshold for beneficial effects appears to be a brain temperature less than 36 °C (CLARK *et al.*, 1996). Clinically feasible brain cooling methods include a head hood or helmet with chemical cooling, head immersion in ice water, nasophyaryngeal cooling after tracheal intubation, intravascular perfusion, and peritoneal cold lavage (MARION *et al.*, 1996).

In this study, we simulated the temperature field achieved by selectively cooling the brain surface. The results of the study suggest that simply packing ice outside the brain and neck surface could lead to an average brain tissue temperature at least several degrees lower than the body core temperature. Thus it is feasible to induce mild brain hypothermia using selective cooling of the brain and neck surface, whereas this may not be effective to achieve moderate hypothermia (28–32 °C).

Our model has several limitations. It is not capable of predicting the transient behaviour of the temperature distribution in the brain during the hypothermia treatment. The real shape of the brain is not exactly hemispherical. However, selecting appropriate dimensions of the brain size can yield a reasonable hemisphere that matches the real cerebral volume and the average radial dimension and thus minimises the error. The uniform skin temperature used in our model can be viewed as an average value of T_{skin}, as, in the real situation, the surface temperature of the scalp may not be uniform. In addition, spatial variation in the thermal properties and blood perfusion in the brain tissue can also affect the temperature distribution in the brain. Other errors are mainly inherited from the accuracy of

Table 3 Effects of T_{skin} and T_a on location of $T_{bt,avg}$ beneath brain tissue surface (mm)

	T_{skin}, °C		0	10	20	30
Adult	$T_a = 37$ °C	$\omega_{bt} = 50\,\text{ml}\,\text{min}^{-1}\,100\,\text{g}^{-1}$	7.52 mm	7.52 mm	7.52 mm	7.50 mm
	$T_a = 35$ °C		7.52 mm	7.52 mm	7.52 mm	7.51 mm
Infant	$T_a = 37$ °C	$\omega_{bt} = 50\,\text{ml}\,\text{min}^{-1}\,100\,\text{g}^{-1}$	5.91 mm	5.91 mm	5.90 mm	5.89 mm
	$T_a = 35$ °C		5.91 mm	5.91 mm	5.90 mm	5.89 mm

Table 4 Effect of ω_{bt} on location of $T_{bt,avg}$ beneath brain tissue surface (mm)

ω_{bt}, ml min^{-1} 100 g^{-1}	25	50	100	50 $3^{(T-T_a)/10}$
Adult, $T_a = 37\,°C$	8.92 mm	7.52 mm	5.59 mm	8.14 mm
Infant, $T_a = 37\,°C$	6.82 mm	5.91 mm	4.82 mm	6.98 mm

the Pennes bioheat equation. The simulation in the brain may be more accurate if the Pennes perfusion source term is modified by introducing a 'correction coefficient' as was analysed in the muscle tissue (WEINBAUM *et al.*, 1997). However, the correction coefficient has not been evaluated in brain tissue. Further, like other continuum models, the Pennes equation cannot be used to predict point-to-point temperature variation in the vicinity of large blood vessels (KOLIOS *et al.*, 1998).

Our results show that the temperature of the arterial blood should not deviate too much (~0.2 °C) from the deep brain tissue temperature. However, when the head surface is cooled during hypothermia treatment, the arterial blood temperature is no longer a reliable indicator of the average brain tissue temperature. Temperature difference in the superficial brain tissue can be up to 20 °C, so that the cerebral cooling is not uniform. This agrees well with the experimental observation that large temperature variations exist in the brain tissue (KULUZ *et al.*, 1992; MIYAZAWA and HOSSMANN, 1992). Our theoretical simulation also predicts that the thickness of the brain tissue layer with temperature variations was approximately 17 mm in both adults and infants. It agrees well with the direct intra-operative measurements showing that the brain tissue temperature is essentially the same at 20 mm beneath the cortical surface (STONE *et al.*, 1997).

It is not surprising to see relatively uniform temperature distribution in the deep brain region, as large blood perfusion in the brain effectively transfers heat from the inside to the surface via blood circulation. Our simulation indicates that the temperature variation within the brain tissue is larger when the blood perfusion rate is smaller. During hypothermia, the cerebral blood flow can increase or decrease with decreased tissue temperature. It is well accepted that cerebral metabolic heat generation is affected by hypothermia, which produces a 7% reduction in cerebral metabolic rate for oxygen with every 1 °C reduction in brain temperature. If the cerebral blood flow is coupled with the local cerebral metabolism, hypothermia can result in decreased cerebral blood perfusion, especially in the superficial region during head surface cooling.

Our model simulated the temperature distribution with temperature-dependent ω_{bt} and found that it further lowers the average brain tissue temperature compared with that with uniform ω_{bt}. Some studies suggested that the protective effect of hypothermia is associated with its ability to reduce cerebral blood flow, which can be induced by the increased blood viscosity in small cerebral vessels (THORESEN and WYATT, 1997). However, experimental measurements of CBF by KULUZ *et al.* (1992) indicated an elevation of CBF during hypothermia. It seems that the proportional relationship between CBF and local metabolic heat generation can be uncoupled during hypothermia. This may be owing to the direct vascular effect of cerebral hypothermia (OGURA *et al.*, 1991) that decreases vascular resistance in a way that is independent of local metabolism. In addition, anaesthetics can alter the local CBF. It has been reported that, in pertobarbital-anaesthetised dogs, the CBF was profoundly decreased (WASS *et al.*, 1998) and subsequently caused a decrease in brain temperature (VERLOOY *et al.*, 1995). Whether the vascular response is an 'on or off' phenomenon or is described as being directly related to the local temperature, is still to be investigated.

Brain size strongly affects the effectiveness of selective cooling of the head surface. A surface cooling temperature of 20 °C and 0 °C in infants and adults, respectively, will result in the same cooling effect in $T_{bt,avg}$. A smaller brain size, such as in infants, results in a lower average brain tissue temperature and helps to maintain better cerebral hypothermia. The animal models currently used in clinical studies also have smaller brains than those of typical adults. The experimental results on smaller animals thus may not be transferable to human adults. The protective effects associated with those animal models may be due to the lower brain tissue temperature achieved in the clinical studies. To achieve the same protection in human brains, a much lower surface temperature is needed in comparison with the animal models.

In conclusion, using the Pennes bioheat transfer model we have shown that

(*a*) selective cooling of the brain surface results in a large temperature gradient within the superficial region of the brain tissue
(*b*) it is feasible to induce mild hypothermia, and this method is more effective when the brain size is smaller and the CBF is lower
(*c*) the temperature sensor should be placed 7.5 mm and 5.9 mm beneath the brain tissue surface for adults and infants, respectively, to monitor continuously the volumetric-averaged brain tissue temperature.

Results from this study are believed to help us gain a better understanding of the temperature distribution in the brain and thus avoid misinterpretations of temperature-sensitive pathological processes. It provides information on how deeply an intracerebral thermal probe must be embedded to obtain a representative measurement of brain temperature. In a situation where direct monitoring of the brain temperature is not available, the simulated results still enable clinicians to approximate the extent of selective cooling of the head surface and to improve cerebral protective therapy. Finally, the strong dependence of the cooling on the local blood perfusion suggests that further experimental study of the blood flow response to cooling is necessary for future modelling.

Acknowledgments—This work was supported by a UMBC Summer Faculty Fellowship and by the American Heart Association (grant 0160320U).

References

BARONE, F. C., FEUERSTEIN, G. Z., and WHITE, R. F. (1997): 'Brain cooling during transient focal ischaemia provides complete neuroprotection', *Neurosci. Biobehav. Rev.*, **21**, pp. 31–44

BLINKOV, S. A., and GLEZER, I. I. (1968): 'Human brain in figures and tables: a quantitative handbook' (Plenum Press, New York, 1968)

CLIFTON, G. L., JIANG, J. Y., and LYETH, B. G. (1991): 'Marked protection by moderate hypothermia after experimental traumatic brain injury', *J. Cereb. Blood Flow Metab.*, **11**, pp. 114–121

CLARK, R. S. B., KOCHANEK, P. M., MARION, D. W., SCHIDING, J. K., WHITE, M., PALMER, A. M., and DEKOSKY, S. T. (1996): 'Mild posttraumatic hypothermia reduces mortality after severe controlled cortical impart in rats', *J. Cereb. Blood Flow Metab.*, **16**, pp. 253–261

DEXTER, F., and HINDERMAN, B. J. (1994): 'Computer simulation of brain cooling during cardiopulmonary bypass', *Ann. Thorac. Surg.*, **57**, pp. 1171–1179

KOLIOS, M. C., WORTHINGTON, A. E., SHERAR, M. D., and HUNT, J. W. (1998): 'Experimental evaluation of two simple thermal models using transient temperature analysis', *Phys. Med. Biol.*, **43**, pp. 3325–3340

KULUZ, J. W., GREGORY, G. A., YU, A. C. H., and CHANG, Y. (1992): 'Selective brain cooling during and after prolonged global ischemia reduces cortical damage in rats', *Stroke*, **23**, pp. 1792–1797

JIANG, J. Y., LYETH, B. G., CLIFTON, G. L., JENKINS, L. W., HAMM, R. J., and HAYES, R. L. (1991): 'Relationship between body and brain temperature in traumatically brain-injured rodents', *J. Neurosurg.*, **74**, pp. 492–496

LYONS, B. E., SAMULSKI, T. V., COX, R. S., and FESSENDEN, P. (1989): 'Heat loss and blood flow during hyperthermia in normal canine brain. I: empirical study and analysis', *Int. J. Hypertherm.*, **5**, pp. 225–247

MARION, D. W., LEONOV, Y., GINSBERG, M., KATZ, L. M., KOCHANEK, P. M., LECHLEUTHNER, A., NEMOTO, E. M., OBRIST, W., SAFAR, P., STERZ, F., TISHERMAN, S. A., WHITE, R. J., XIAO, F., and ZAR, H. (1996): 'Resuscitative hypothermia', *Crit. Care Med.*, **24**, pp. s81–s89

MARION, D. W. (1997): 'Treatment of traumatic brain injury with moderate hypothermia', *N. Engl. J. Med.*, **336**, pp. 540–546

MELLERGARD, P., NORDTROEM, C.-H., and CHRISTENSSON, M. (1990): 'A method for monitoring intracerebral temperature in neurosurgical patients', *Neurosurgery*, **27**, pp. 654–657

MIYAZAWA, T., and HOSSMANN, K.-A. (1992): 'Methodological requirements for accurate measurements of brain and body temperature during global forebrain ischaemia of rat', *J. Cereb. Blood Flow Metab.*, **12**, pp. 817–822

NELSON, D. A., and NUNNELEY, S. A. (1998): 'Brain temperature and limits on transcranial cooling in humans: quantitative modeling results', *Eur. J. Appl. Physiol.*, **78**, pp. 353–359

OGURA, K., TAKAYASU, M., and DACEY, R. G. (1991): 'Effects of hypothermia and hyperthermia on the reactivity of rat intracerebral arterioles *in vitro*', *J. Neurosurg.*, **75**, pp. 433–439

OLSEN, R. W., HAYES, L. J., WISSLER, E. H., NIKAIDOH, H., and EBERHART, R. C. (1985): 'Influence of hypothermia and circulatory arrest on cerebral temperature distributions', *ASME J. Biomech. Eng.*, **107**, pp. 354–360

PENNES, H. H. (1948): 'Analysis of tissue and arterial blood temperatures in the resting human forearm', *J. Appl. Physiol.*, **1**, pp. 93–122

RUMANA, C. S., GOPINATH, S. P., UZURA, M., VALADKA, A. B., and ROBERTSON, C. S. (1998): 'Brain temperature exceeds systemic temperature in head-injured patients', *Crit. Care Med.*, **26**, pp. 562–567

SAMULSKI, T. V., COX, R. S., LYONS, B. E., and FESSENDEN, P. (1989): 'Heat loss and blood flow during hyperthermia in normal canine brain. II: mathematical model', *Int. J. Hypertherm.*, **5**, pp. 249–263

SCHWAB, S., SPRANGER, M., ASCHOFF, A., STEINER, T., and HACKE, W. (1997): 'Brain temperature monitoring and modulation in patients with severe MCA infarction', *Neurology*, **48**, pp. 762–767

SIRIMANNE, E. S., BLUMBERG, R. M., BOSSANA, D., GUNNING, M., EDWARDS, A. D., GLUCKMAN, P. D., and WILLIAMS, C. E. (1996): 'The effect of prolonged modification of cerebral temperature on outcome after hypoxic-ischaemic brain injury in the infant rat', *Pediat. Res.*, **39**, pp. 591–597

STONE, J. G., YOUNG, W. L., SMITH, C. R., SOLOMON, R. A., WALD, A., OSTAPKOVICH, N., and SHREBNICK, D. B. (1995): 'Do standard monitoring sites reflect true brain temperature when profound hypothermia is rapidly induced and reversed?', *Anesthesiology*, **82**, pp. 344–351

STONE, J. G., GOODMAN, R. R., BAKER, K. Z., BAKER, C. J., and SOLOMON, R. A. (1997): 'Direct intraoperative measurement of human brain temperature', *Neurosurgery*, **41**, pp. 20–24

THORESEN, M., and WYATT, J. (1997): 'Keeping a cool head, post-hypoxic hypothermia—an old idea revisited', *Acta Pediatr.*, **86**, pp. 1029–1033

VERLOOY, J., HEYTENS, L., VEECKMANS, G., and SELOSSE, P. (1995): 'Intracerebral temperature monitoring in severely head injured patients', *Acta Neurochir (Wien)*, **184**, pp. 76–78

WASS, C. T., LANIER, W. L., HOFER, R. E., SCHEITHAUER, B. W., and ANDREWS, A. G. (1995): 'Temperature changes of $\geq 1\,^{\circ}C$ alter functional neurologic outcome and histopathology in a canine model of complete cerebral ischemia', *Anesthesiology*, **83**, pp. 325–335

WASS, C. T., WAGGONER, J. R., CABLE, D. G., SCHROEDER, D. R., and LANIER, W. L. (1998): 'Selective convective brain cooling during normothermic cardiopulmonary bypass in dogs', *J. Thorac. Cardiovasc. Surg.*, **115**, pp. 1350–1357

WEINBAUM, S., XU, L. X., ZHU, L., and EKPENE, A. (1997): 'A new fundamental bioheat equation for muscle tissue. Part I: blood perfusion term', *ASME J. Biomech. Eng.*, **121**, pp. 1–12

XU, X., TIKUISIS, P., and GIESBRECHT, G. (1999): 'A mathematical model for human brain cooling during cold-water near-drowning', *J. Appl. Physiol.*, **86**, pp. 265–272

ZHU, L., and XU, L. X. (1999): 'Evaluation of the effectiveness of transurethral radio frequency hyperthermia in the canine prostate: temperature distribution analysis', *ASME J. Biomech. Eng.*, **121**, pp. 584–590

ZHU, L. (2000): 'Theoretical evaluation of contributions of both radial heat conduction and countercurrent heat exchange in selective brain cooling in humans', *Ann. Biomed. Eng.*, **28**, pp. 269–277

Author's biography

LIANG ZHU received her BS from the University of Science and Technology of China, Anhui, China, in 1988, and PhD from the City University of New York, New York, in 1995. She has been an Assistant Professor in the Department of Mechanical Engineering at the University of Maryland Baltimore County since 1998. Her research is focused on the fundamental heat transfer mechanism in biological systems and its clinical applications.